

Report

**P-16-07**

January 2018



# Investigation of alternatives to the buffer protection

**Peter Eriksson**

SVENSK KÄRNBRÄNSLEHANTERING AB

SWEDISH NUCLEAR FUEL  
AND WASTE MANAGEMENT CO

Box 3091, SE-169 03 Solna  
Phone +46 8 459 84 00  
skb.se

SVENSK KÄRNBRÄNSLEHANTERING



ISSN 1651-4416

**SKB P-16-07**

ID 1518994

January 2018

# **Investigation of alternatives to the buffer protection**

Peter Eriksson, Svensk Kärnbränslehantering AB

A pdf version of this document can be downloaded from [www.skb.se](http://www.skb.se).

© 2018 Svensk Kärnbränslehantering AB



## Abstract

According to the current installation sequence a canister it will be placed in the deposition hole together with the buffer for up to three months before the backfill is installed on top of the deposition hole. During this time period the buffer is subjected to heat and moisture which could make the buffer blocks to crack. This could cause problems in fulfilling the intended initial state. Currently the buffer is protected by a rubber sheet but there could be a problem to remove this. Therefore it is advantageous if the installation of the buffer could be done without this.

Two different alternative ways of protecting the buffer during the first three months before the backfill has been installed have been investigated. These two alternatives are:

- Controlled atmosphere.
- Coating of the blocks.

In controlled atmosphere the relative humidity in the outer gap between the buffer and the wall of the deposition hole is controlled. The idea is to let the bentonite be in equilibrium with the relative humidity in the air in the outer gap. However, it has been shown that it is difficult to keep an even relative humidity due to the temperature gradients in axial direction over the deposition hole. This alternative gives only slightly less water redistribution in the buffer then the current solution. Therefore it is concluded that this small improvement is not worth the extra complexity with fans, dehumidifier and control electronics.

In coating of the blocks the block are protected by a thin layer of a material that prevents water from leaving or entering the block. Tests have been done and they show that most of the coatings lose their function very quickly. The exception is a coating with polyethylene which has very low permeability and high ductility. However, if the coating is water tight the water content will increase close to the coating and this could cause the block to expand and crack. This cracking could cause the buffer stack to heave which could cause problems with fulfilling the intended initial state. The coating of block does therefore not perform better than the current solution.

# Sammanfattning

Enligt den nuvarande installationssekvensen så kommer kapseln att vara placerad i sitt deponeringshåll tillsammans med bufferten upp till tre månader innan återfyllningen installeras över deponeringshålet. Under denna tid utsätts bufferten för en termisk gradient samt fukt från berget som kan göra att blocken spricker. Detta kan i sin tur göra så att det blir problem med att uppnå det eftersträvade initialtillståndet. I dagens utformning så skyddas bufferten av ett buffertskydd men det skulle kunna uppstå problem vid bortmontering av detta. Det vore därför en fördel om buffertskyddet kunde bytas ut mot någon bättre lösning för att minska sprickbildningen i blocken.

Två olika lösningar för att skydda bufferten under de tre första månaderna har utretts. Dessa alternativ är:

- Kontrollerad atmosfär.
- Beläggning av block.

I alternativet kontrollerad atmosfär kontrolleras och justeras den relativa fuktigheten i den yttre spalten och idén är att hålla den relativa fuktigheten på en nivå där den är i jämvikt med buffertblocken. Dock har det visat sig svårt att hålla en jämn relativfuktighet i spalten på grund av den termiska gradienten i axiell riktning som finns i hålet. Detta alternativ ger endast en liten förbättring jämfört med den befintliga lösningen. Bedömningen är att de små förbättringarna inte uppväger den ökade komplexiteten med fläktar, avfuktare och styrelektronik.

Vid beläggning av block så skyddas blocken av ett tunt lager av ett material som hindrar vattnet från att tas upp eller avges från buffertblocket. Tester som har gjorts har visat att de flesta beläggningarna tappar sin effekt efter ett kort tag. Undantaget är beläggningen av polyeten som har väldigt låg vattengenomsläpplighet och är väldigt duktil. Men om beläggningen är tät så kan det leda till att vattenkvoten ökar närmast beläggningen och det kan i sin tur få blocket att expandera och spricka. Denna uppsprickning kan få blockstapeln att häva sig uppåt vilket i sin tur kan ge problem att uppnå det eftersträvade initialtillståndet.

# Contents

<b>1</b>	<b>Introduction</b>	7
1.1	Background	7
1.2	Purpose and objectives	7
1.3	Scope	7
<b>2</b>	<b>Evaluation criteria's</b>	9
<b>3</b>	<b>Cracking of blocks</b>	11
3.1	Shrinkage curve	11
3.2	Test of behaviour of drying cracks	11
3.2.1	Purpose	11
3.2.2	Test layout	12
3.2.3	Sampling	13
3.2.4	Water content and density	13
3.2.5	Fracture development	13
3.2.6	Model of crack depth	14
<b>4</b>	<b>Controlled atmosphere</b>	17
4.1	General description	17
4.2	Testing of the method	17
4.2.1	Test setup	17
4.2.2	Running the test	17
4.2.3	Results	19
4.3	Modelling of controlled atmosphere	19
4.3.1	Method	19
4.3.2	Constitutive equations	20
4.3.3	Modelled Air flow in the test	22
4.3.4	Heat flow modelling	22
4.4	Modelling of a real case	27
4.5	Possible improvements	29
<b>5</b>	<b>Coating of blocks</b>	31
5.1	General description	31
5.2	Materials tested	31
5.3	Coating of the samples	32
5.4	Testing of the coatings	33
5.5	Modelling of a buffer stack with coating	34
<b>6</b>	<b>Conclusions</b>	37
6.1	Controlled atmosphere	37
6.2	Coating of blocks	37
	<b>References</b>	39





# 1 Introduction

## 1.1 Background

According to SKB's reference method for disposal of spent nuclear fuel, canisters containing the spent fuel are deposited 500 meters down in the bedrock surrounded by swelling clay. Furthermore, the deposition tunnel is backfilled with blocks and pellets. The clay is installed in form of blocks and pellets. The blocks in the deposition hole are called buffer blocks and the blocks in the deposition tunnel are called backfill blocks.

After the deposition tunnel has been excavated and deposition holes have been drilled the material in the tunnel is installed in the following sequence:

1. Installation of the buffer protection and bottom plate in the entire deposition tunnel.
2. Installation of buffer and canister for the entire deposition tunnel.
3. Filling pellets in the deposition hole and backfilling of the deposition tunnel.
4. Construction of a plug.

A consequence of this sequence is that the buffer will be standing for three months (Wimelius and Pusch 2008) before the pellet is filled in the gap between the buffer and the rock wall in the deposition hole and the deposition tunnel is backfilled. During this time the heat which is generated in the canister and moisture from the rock will affect the buffer blocks. Therefore the blocks need to be protected during this time. In the reference design this is done with a rubber protection sheet called buffer protection. This buffer protection is designed to protect the blocks from moisture from the rock. However, it does not protect the blocks from the heat gradient which will redistribute the moisture in the blocks causing stresses in the blocks. These stresses will cause the block to crack and if the cracks are too large material can fall into the outer gap causing problems when removing the buffer protection, potentially leading to pieces being left in the deposition hole.

Because of the possible problems with the buffer protection two alternatives to the buffer protection have earlier been identified which need to be investigated to get a better base for decision of what method will be used to protect the buffer during the first 90 days.

## 1.2 Purpose and objectives

The purpose of this work is to investigate alternative, without buffer protection, solutions to protect the buffer during the installation time. Concepts should be developed for promising solutions that are able to protect the buffer during the three month period before the deposition tunnel is backfilled. The concept should be able to automate the removal and reduce the risk of material being unintentionally left in the deposition hole.

## 1.3 Scope

In this work two alternatives to protect the buffer during installation has been investigated. These two alternatives are:

1. Controlled atmosphere.
2. Coating of blocks.

These two alternatives were earlier identified as possible solutions to replace the buffer protection used in the current reference design. The solutions will be evaluated to find out how they perform during the three month storage in the deposition hole together with a hot canister. The redistribution of water will be modelled to get some indication if and how the buffer cracks.



## 2 Evaluation criteria's

To be able to evaluate how well a system for protection of the buffer works some criteria need to be established. The buffer blocks can start to crack if water content change locally. The change in water content can be caused by thermal gradients that redistribute the water in the buffer, inflows and condensation from air surrounding the buffer. In general, cracking of the buffer blocks is not a problem. However, if parts of the buffer block falls into the outer gap before it is filled with pellets there can be problem removing equipment used to protect the buffer. Another thing is that cracking might cause the buffer to heave if the cracks are oriented in the horizontal direction due to air is then introduced into the buffer reducing its density. If the heave is to big there would be problems to install the backfill and the density of the buffer may become too low. Therefore the following criteria's will be used to compare the alternatives.

- Reduce cracking so that no parts of the buffer will fall into the outer gap causing problems when removing the equipment and filling of pellets.
- Restrict heaving.



### 3 Cracking of blocks

#### 3.1 Shrinkage curve

The buffer blocks are susceptible to cracking when the water content changes. This is because the water uptake or drying of the blocks causes volume changes in the material.

To get an understanding of the volume changes of the bentonite during drying, small blocks were compacted of MX-80 bentonite. The blocks were then dried slowly in a climate chamber to avoid cracking. The density was measured at regular intervals and the water content was calculated. Results from the measurements can be seen in Figure 3-1.

An empirical expression to predict the density changes during drying is suggested, Equation (3-1), which seems to work well in the water content interval 5-30 %.

$$\rho = \frac{\rho_s}{\left(1 + \frac{\rho_s}{\rho_w} w\right) \left(1 + E0 e^{-\frac{6}{E0} w}\right)} \quad (3-1)$$

Were:

$\rho_s$  is the grain density (2800 kg/m<sup>3</sup>),

$\rho_w$  is the density of water (1000 kg/m<sup>3</sup>),

w is the gravimetric water content (mass of water divided with dry mass),

E0 is a constant that describes the initial porosity.

#### 3.2 Test of behaviour of drying cracks

##### 3.2.1 Purpose

When the buffer blocks takes up water or dry they will crack. When the blocks take up water from the outer diameter, the blocks tend to crack in the horizontal direction (Sandén and Börgesson 2010) (Åberg 2009) which causes heaving and result in parts of the block falling out into the outer gap.

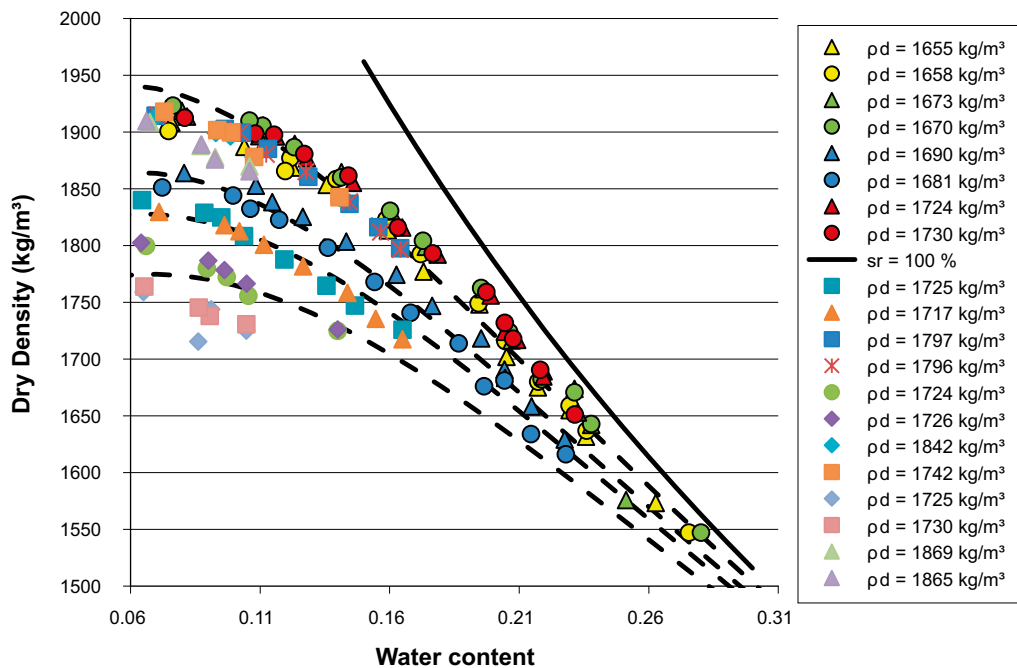


**Figure 3-1.** Volume change of bentonite during drying. The initial dry density is shown in the legend. Dashed lines is empirical model Equation (3-1).

Even though there are no pellet in the alternatives tested in this report there could still condensate water in parts of the buffer that are cooler causing the same type of horizontal cracks. In the deposition hole, however, it is expected that there will be mainly drying conditions due to the thermal gradient that forms over the outer slot. Therefore, some tests were done to get a better understanding of how the blocks crack during the drying process. The purpose was to see if the depth of the crack could be predicted from the water content profiles. If this information is known it is easier to evaluate how the buffer reacts to drying caused by heat generated from the canister.

### 3.2.2 Test layout

Six blocks were placed in an environmental chamber with controlled temperature and humidity. The blocks were placed in two stacks with three blocks in each, Figure 3-2. Between each block there was a rubber mat i.e. the blocks could only absorb water from the exposed periphery. The rubber mats also prevented any water transport from block to block. Rubber mats were also placed at the top and bottom surfaces of the stacks. A steel plate was placed on the top of each stack to secure close contact between rubber and block.

The initial relative humidity in the climate chamber was 75 % and was then lowered with 3 % each day while the temperature was approx. constant, see Figure 3-3. The starting relative humidity was chosen to be close to the equilibrium value for the initial water content in the block to reduce big gradients in water content in the beginning of the test. The blocks were removed at different times and then analyzed regarding water content and density distribution in the radial direction. The blocks were removed after 1, 2, 4, 8, 16 and 21 days.



*Figure 3-2. Photo showing the blocks after emplacement in the climate chamber.*

### 3.2.3 Sampling

After removal of a block from the climate chamber, a visual inspection of each block was made and possible fractures documented by photo. An example of how such a photo could look is shown in Figure 3-4.

The bentonite sampling was made by sawing out a cross section of the block (approx. 30 by 30 by 175 mm) across the center of the block. The 10 mm closest to top and bottom surface were also sawed off. The resulting section was then sliced into 4-5 mm thin samples. These samples were divided into two parts one for water content measurement and the other for determination of the bulk density. The water content was determined by drying the sample at 105 °C for 24 h and the density was determined by submerging the sample into paraffin oil, with a known density, while weighing the sample. The radial positions have been calculated from the thickness of the sample and the width of the saw (calculated from the total length of samples and the initial length). The reported positions represent the center of each bentonite sample.

### 3.2.4 Water content and density

The results from the determinations of water content and dry density are provided in Figure 3-5 and 3-6 together with results from modelling of the test. The modeling is done with the equations in Section 4.3.2 with boundary pressure and vapor concentration set to equilibrium with the surrounding air. The results from the sampling of the reference block (day 0) is also shown in the graphs.

The water content was stable during the first two days but started to noticeably drop at the block periphery at day 4 and at day 16 the change had reached the center of the block. In the last block (day 21), the water content had dropped somewhat further.

The determinations of the dry density show that there is a very small influence of the climate on the dry density during the first four days. The block that was removed from the climate chamber after 8 days was, however, evidently influenced of the drying process and the samples closest to the block periphery had obviously higher density than the inner parts due to the shrinkage. This trend continued also for the blocks that were sampled after 16 and 21 days respectively.

### 3.2.5 Fracture development

Immediately after emplacement of the six blocks in the climate chamber, some small cracks could be seen on the block surfaces. These cracks were probably only present at the surface and they disappeared within one day. No fractures were detected on the two first blocks removed from the climate chamber (after 1 day and 2 days test respectively). The number of fractures increased with exposure time as well as the depth of the cracks and the cracks appeared in the radial direction as seen in Figure 3-7.

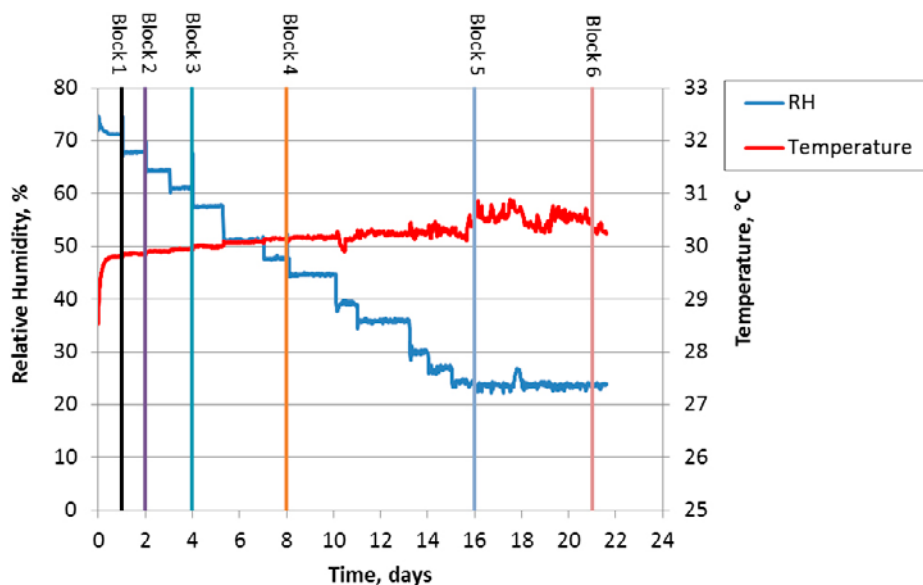
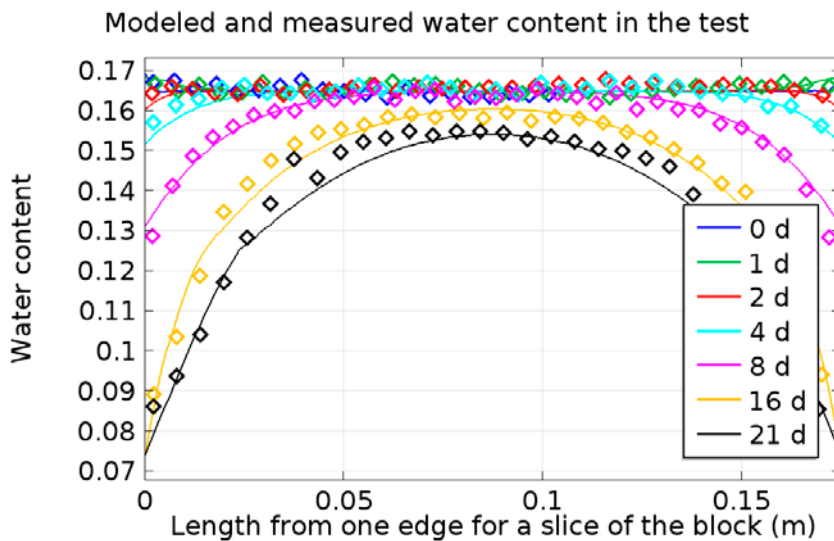


Figure 3-3. Relative humidity and temperature during the test.



**Figure 3-4.** Photo showing cracks. The block has been taken out of the climate chamber after 16 days.



**Figure 3-5.** Water content distribution plotted versus the distance from one block side to the other. The vertical line shows the center of the block. Diamonds are measured results and solid lines are modeled results obtained from modelled water content and Equation (3-1).

### 3.2.6 Model of crack depth

The drying crack seems to be more predictable than cracks that arise due to water uptake. They also seem to always be in the radial direction. Therefore an attempt to find an expression that can predict the depth of the cracks was made. To try and estimate the crack depth during the drying process a simple model is constructed. To simplify the calculations it is assumed that stress in the cracked zone is zero, see Figure 3-8.

This is not completely correct as the cracked zone still have tensions that will try to further open the crack and therefore the model should underestimate the crack depth.



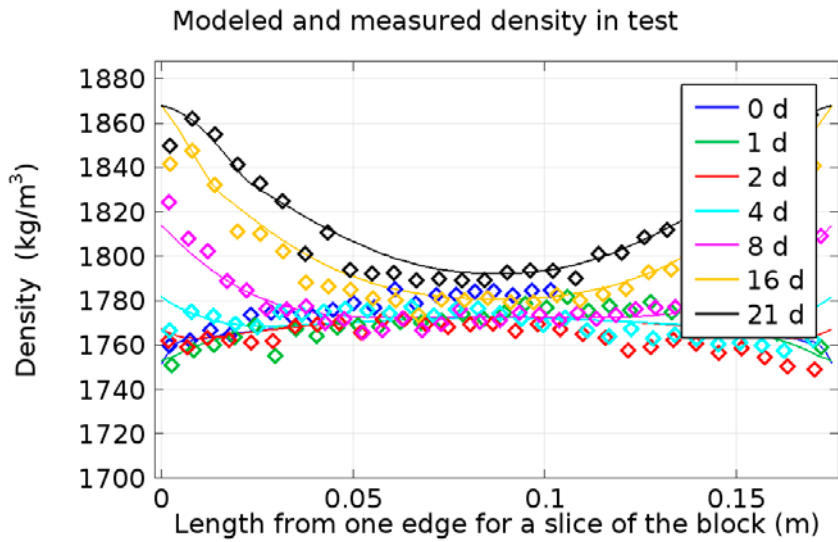


**Figure 3-6.** Dry density distribution plotted versus the distance from one block side to the other. The vertical line shows the center of the block. Diamonds are measured results and solid lines are modeled results.

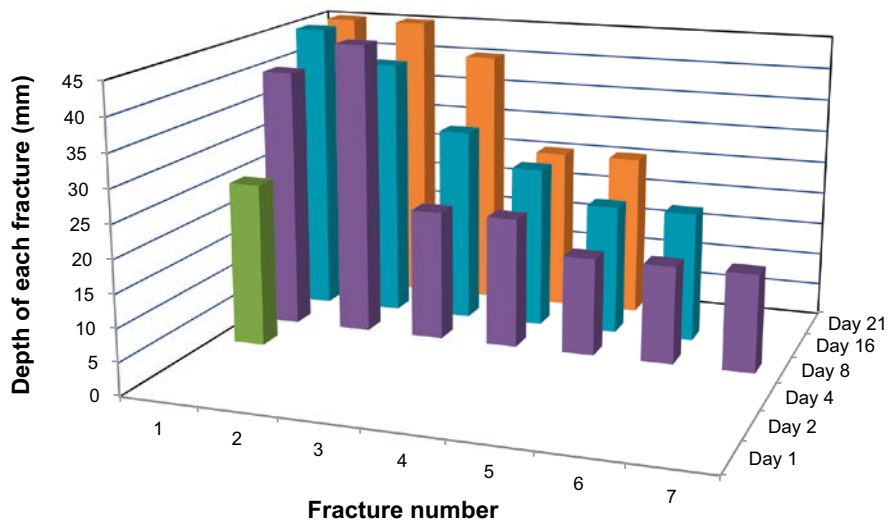


**Figure 3-7.** Graph showing the number of fractures in the different blocks together with the measured depth.

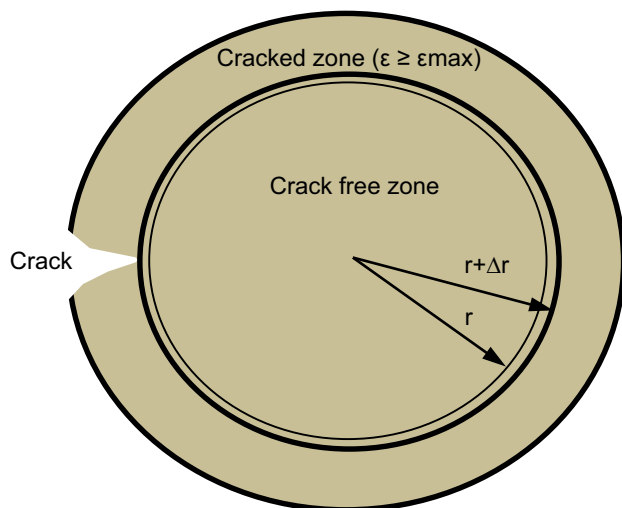


**Figure 3-8.** Schematic figure of the two zones, the crack free zone and the cracked zone.

The strain is estimated by looking at a small radius interval,  $\Delta r$ . By multiplying the radius with the relative volume change of the material an estimation of what radius this interval would have if it was unconstricted. However, the interval is constricted from movement due to swelling/shrinking by the material inside this radius interval. Therefore the actual radius is calculated by integrating all the relative volume changes from the centre to the radius  $r$ . By dividing at actual radius with the unconstricted we will get a strain. The strain in the crack free zone can therefore be estimated according to Equation (3-2) if the cracked zone is neglected.

$$\varepsilon(r) = \frac{\int_0^r \frac{v(r)}{v_0(r)} dr}{r \frac{v(r)}{v_0(r)}} \tag{3-2}$$

Were:

$V(r)$  is the volume,

$V_0(r)$  is the initial volume,

$r$  is the radius.

The relative volume is calculated from the relation,  $\frac{v(r)}{v_0(r)} = \frac{\rho_0(r)}{\rho(r)}$ , were  $\rho(r)$  is taken from Equation (3-1).

The material is considered cracked if Equation (3-3) is fulfilled.

$$\varepsilon \geq \varepsilon_{max} \tag{3-3}$$

$\varepsilon_{max}$  is the strain at failure and can be estimated from beam tests. Beam tests that have been done show a strain at failure is approximately 0.6 % (Sandén et al. 2016). If this criterion is used the maximum crack depth for the test in Section 3.2 can be plotted as a function of time, see Figure 3-9. The blue line is taken from Equation (3-2) where the water content and density profiles of the tests are replicated with finite element modelling. The stepwise increase of crack depth represents the nodes in the model. The model underestimates the crack depth especially in the beginning of the test but this is expected. The model cannot describe number of cracks if this is needed the model needs to be developed further.

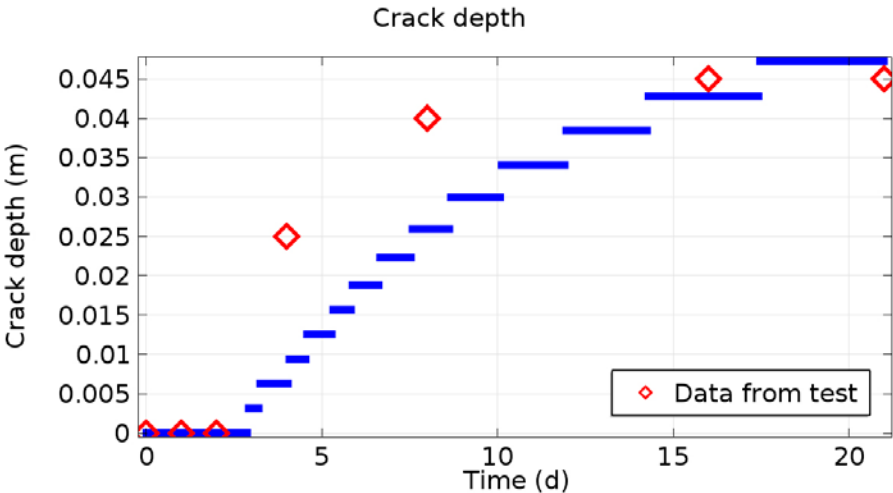


Figure 3-9. Model of how the maximum crack depth varies with time compared to the measured data (red dots are measured data).

## 4 Controlled atmosphere

### 4.1 General description

The idea with this method is to keep the relative humidity in the outer gap constant at a level where it is in equilibrium with the buffer at the desired water content. At the water content 17 % this equilibrium is approximately at 70 % relative humidity, as seen in Figure 4-6. When the water vapour is pushed from the buffer into the outer gap the relative humidity increases therefore water vapour needs to be removed. Since the relative humidity is also dependent on temperature it is also important to try to get an even temperature in the gap.

To achieve this, air is circulated in the outer gap to get an even temperature and the relative humidity is constantly controlled with a dehumidifier. To reduce the thermal gradient in the axial direction, since even a small temperature difference can make a large change in relative humidity, a high airflow in the outer gap is desirable.

To get air down to the bottom of the deposition hole the air is pumped down with hoses. The air then rises to the top where it will leave the outer gap. The air is then lead through a dehumidifier where the relative humidity is controlled to a value suitable for the buffer before it is pumped down to the bottom of the deposition hole again. The idea is to remove the same amount of water that is evaporated from the rock wall and thereby keeping the amount of water in the deposition hole constant. The dehumidifiers are good at controlling the relative humidity when water is removed but it cannot add moisture if the air gets to dry, therefore it is important to seal the system so that the leakage of water vapour is less than the water evaporated from the rock wall.

### 4.2 Testing of the method

#### 4.2.1 Test setup

In order to evaluate the method and get more data that can be used to improve and test models of the system a full scale test was done. To get the test as realistic as possible the test was done in a deposition hole at Äspö HRL. The deposition hole is in full-scale with a diameter of approximately 1750 mm and a depth of approximately 8 m. The inflow in the deposition hole had earlier been measured and is in the order of  $10^{-4}$  l/m/min. A canister with heaters (1700 W) was also used to get as realistic heat conditions as possible. However, the buffer blocks were replaced with concrete blocks, which has a diameter of 1650 mm, to simplify handling during assembly and disassembly of the test. The concrete blocks do not affect the relative humidity in the out gap as much as bentonite would, however, this effect of water evaporation or water absorption by the bentonite will be added in modelling. Test was originally planned to be setup as in Figure 4-1. But an extra fan was later added to get a high enough air flow which is shown in Figure 4-2. Due to difficulty of assembly the concrete blocks was assembled eccentric which meant that the inlet hoses could not be placed symmetrically.

#### 4.2.2 Running the test

The test started off with a short period of 2 days with lower power, 500 W, to test the equipment. After that the power was raised to 1700 W. The test can be divided into three stages where the system was controlled in different ways.

1. Manual control of the dehumidifier (day 1–day 13).
2. The humidifier was controlled with sensor 1 (day 13–day 17).
3. The dehumidifier was controlled with sensor 2 (day 17–end of test).



Figure 4-1. The top part of the deposition hole used for the test.

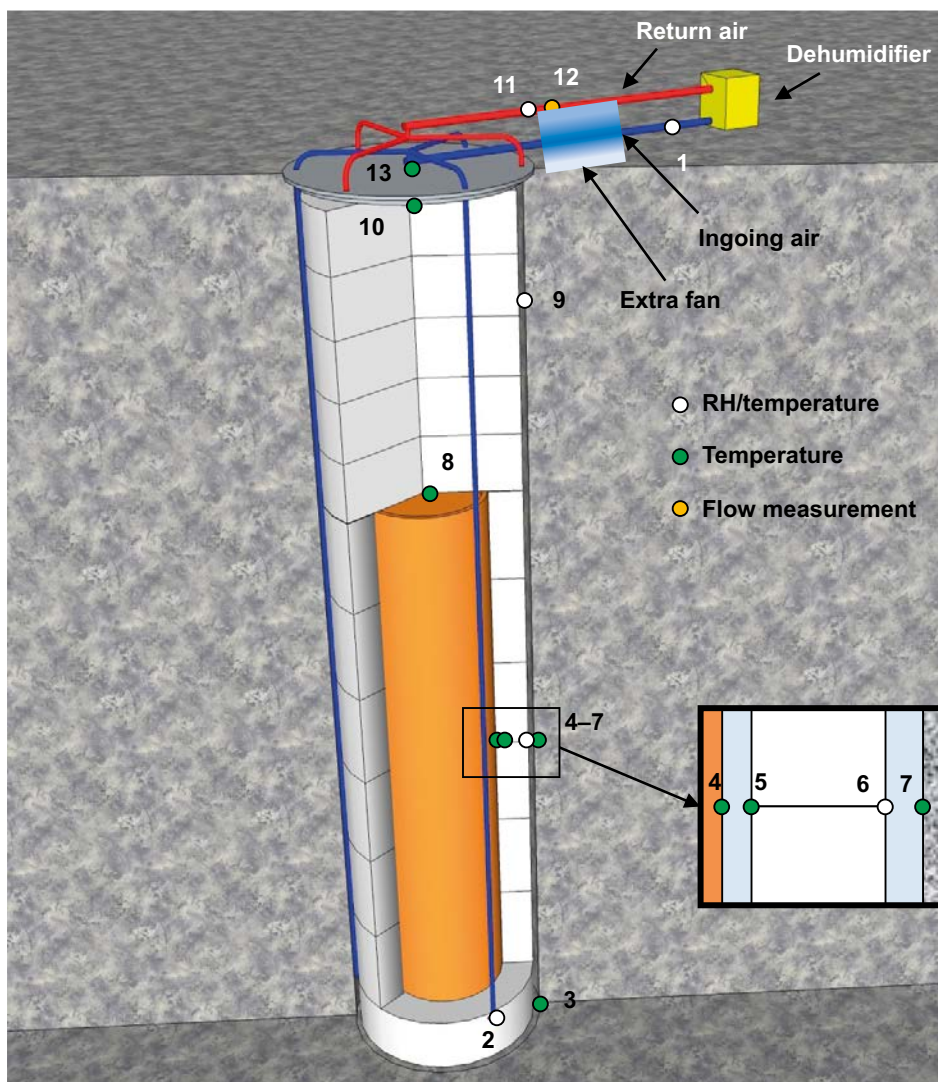


Figure 4-2. Sketch of the test setup and sensor placement.

During the test three sensors were broken. The number 6 sensor was broken from the start and after approximately 31 days sensor 9 and 11 was broken. Sensor 11 could be replaced but sensor 6 and sensor 9 could not be reached. Therefore replacements were lowered down into the outer gap. These sensors could not be positioned very well and therefore it is not known how far from the concrete blocks they were placed. Also sensor 6 replacement was placed in a slightly different angle, therefore the sensor is in the report renamed to sensor 6\*. This is important to note as the blocks were assembled eccentric and therefore the air flow conditions will change depending on where the sensor is placed.

### 4.2.3 Results

When the power was turned on the temperature starts to rise, Figure 4-3 and Figure 4-5. The temperature of the canister increased to approximately 64 °C at the end of the test. The temperature between the rock wall and the concrete blocks could not be measured because the new sensor 6\* was placed somewhere in the outer gap. The small temperature difference measured indicates that the sensor ended up close to the rock wall, as seen in Figure 4-3.

When it comes to the relative humidity the result, Figure 4-4, shows that the incoming air flow had an even relative humidity from when the system was controlled on sensor 2. However, there was a drop in relative humidity around 60 days into the test. The air was entering the outer gap close to sensor 2 at approximately 75 % RH. The temperature increased as the air moved upwards and the relative humidity decreased until the air reached the top of the canister. After that the air started to cool down again and the relative humidity increased. When the air reached sensor 9 it reaches 95 % relative humidity. This is a big variation which could have a big impact on the bentonite blocks.

## 4.3 Modelling of controlled atmosphere

### 4.3.1 Method

Due to the fact that the test did not have an even gap since the block was placed eccentric in the deposition hole it was not possible to use a rotational symmetric model. Therefore, a 3D model was needed. To be able to reduce the computation time the problem was divided into two models, one flow model and one thermal model. When the flow model was solved a simplified analytical version was constructed and used in the thermal model.

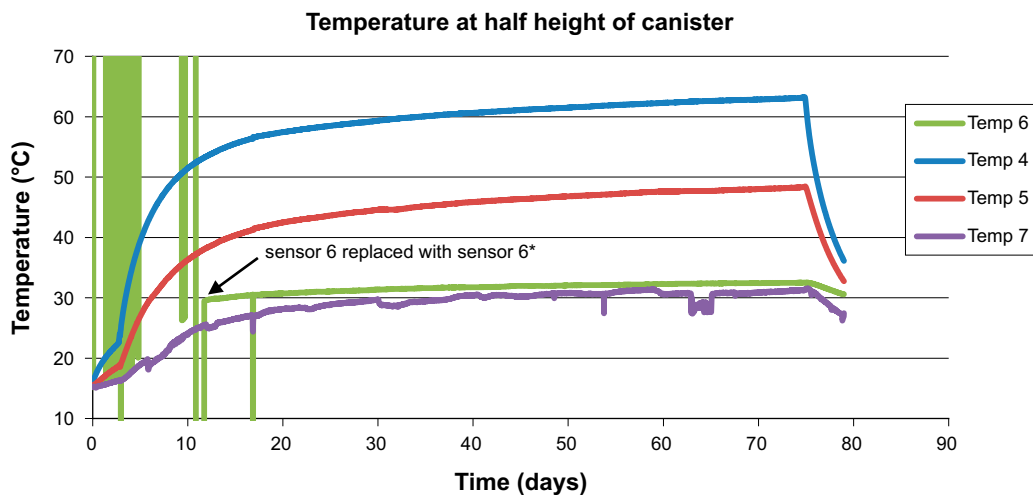


Figure 4-3. Temperature measurements from sensor 4–6.

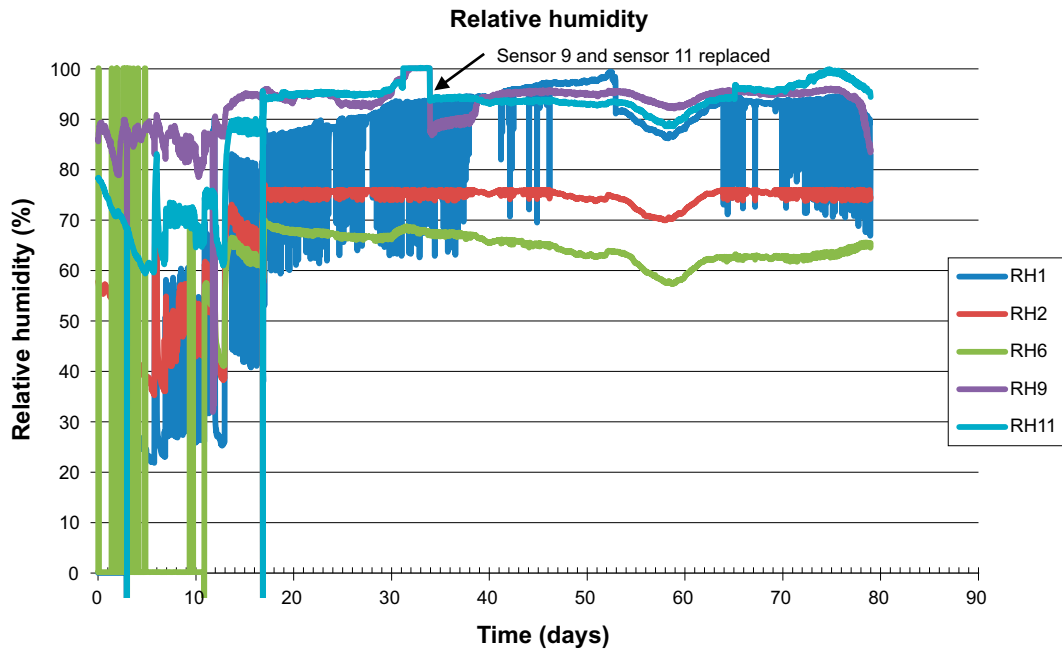


Figure 4-4. Relative humidity data from the test.

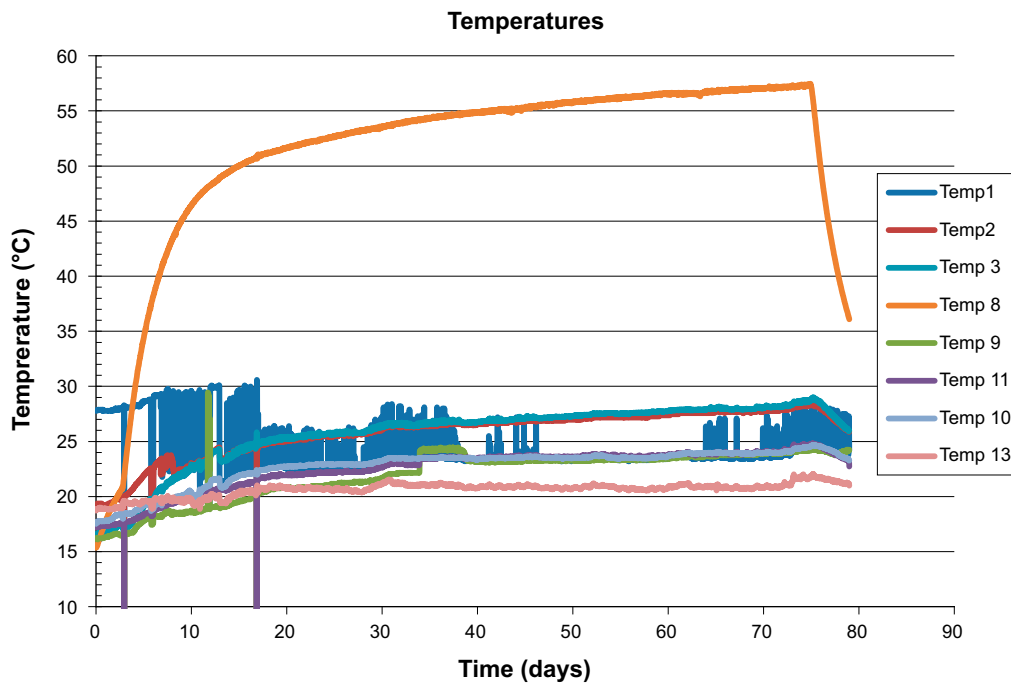


Figure 4-5. Temperature data sensor 1, 2, 3, 8, 9, 11, 10 and 13.

### 4.3.2 Constitutive equations

#### Heat transfer

Heat flow is calculated with the Heat equation, Equation (4-1).

$$\rho C_p \frac{\partial T}{\partial t} + \rho C_p u \nabla T = \nabla(\lambda \nabla T) + Q \quad (4-1)$$

Where  $u$  is the flow velocity calculated with the Navier-Stokes equations,  $Q$  is the heat generated  $C_p$  is Specific heat,  $\lambda$  is the thermal conductivity and  $\rho$  is the density.

In the case where water is evaporating or condensing the heat generated is calculated with Equation (4-2).

$$Q = RH_{vap} \quad (4-2)$$

Where R is the generation of water vapour taken from Equation (4-7) and  $H_{vap}$  is the enthalpy of vaporization for water, 40 650 J/mol.

In the air gaps between the canister and the buffer blocks and between buffer and rock wall thermal radiation is calculated with Stefan Boltzmann law, Equation (4-3).

$$j = \varepsilon \sigma T^4 \quad (4-3)$$

Where  $\sigma$  is Stefan Boltzmann constant, j is the emissive power and  $\varepsilon$  is the emissivity of the material.

### **Transport of liquid water in the bentonite**

To model the transport of liquid water the Richard equation is used, Equation (4-4).

$$\rho \frac{\partial \theta}{\partial p} \frac{\partial p}{\partial t} + \rho \nabla \cdot \left( -\frac{\kappa_s \kappa_r}{\mu} \nabla p \right) = Q_m \quad (4-4)$$

Where  $Q_m$  is a term describing water condensing and evaporating,  $\kappa_s$  is the intrinsic permeability and  $\kappa_r$  is the relative permeability.

To have mass balance the water condensate needs to be the same amount as is lost in vapor,  $Q_m = -R \cdot M_{water}$ , where  $M_{water}$  is the mol weight of water, 0.018 kg/mol.

The retention curve is calculated from Equation (4-5) and a comparison with modelled values can be seen in Figure 4-6.

$$\theta = \frac{0.004}{(1-RH)} + 0,26RH + 0,035wf - 0,035 \quad (4-5)$$

Where wf is a friction force used to capture the hysteresis shown in experimental values. It is calculated from Equation (4-7) and RH is the relative humidity.

$$\ln(RH) = -\frac{pM_{water}}{\rho RT} \quad (4-6)$$

$$\frac{dwf}{dt} = -\frac{2890}{\rho_d} \frac{d\theta}{dt} (|wf| < 1) \quad (4-7)$$

### **Transport of water vapour through diffusion**

The diffusion equation, Equation (4-8), is used model the transport of the water vapour in the bentonite.

$$\frac{\partial c}{\partial t} + \nabla \cdot (-D \nabla c) + u \nabla c = R \quad (4-8)$$

Where c is the concentration of water vapour, D is the diffusion coefficient of water vapour in air and R is a term describing and evaporation and condensation of water vapour.

### **Air movement in pellet filled slot and open air cavities**

The Navier-Stokes equation governs the motion of fluids. In the case of a compressible Newtonian fluid the Navier-Stokes equation can be written according to Equation (4-9).

$$\rho \left( \frac{\partial u}{\partial t} + u \nabla u \right) = -\nabla p_a + \nabla \cdot \left( \mu (\nabla u + (\nabla u)^T) - \frac{2}{3} \mu (\nabla \cdot u) I \right) + F \quad (4-9)$$

Where u is the fluid velocity,  $p_a$  is the fluid pressure,  $\rho$  is the fluid density, F is the external forces and  $\mu$  is the fluid dynamic viscosity.

In the case of an air filled gap the external forces are gravitational, Equation (4-10).

$$F = F_g = -\rho g \quad (4-10)$$

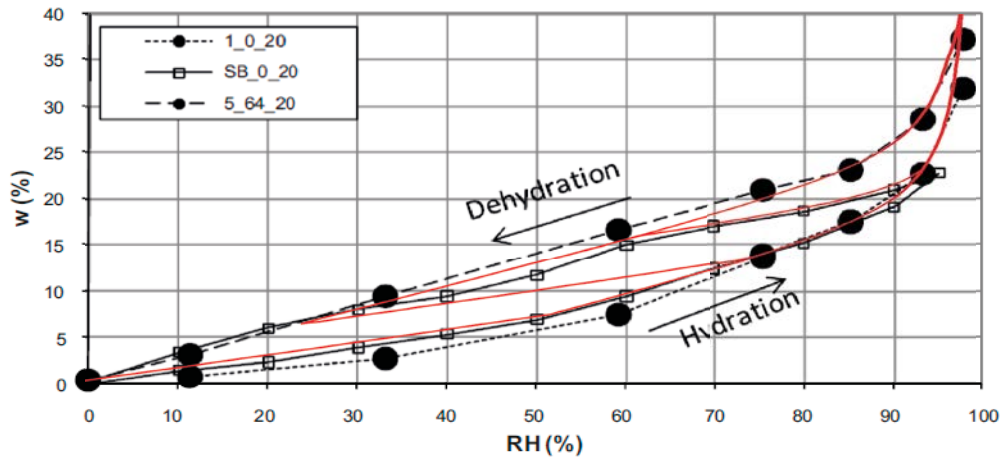


**Figure 4-6.** Measured values compared to model with hysteresis. Measured values taken from Åkesson et al. (2010).

### 4.3.3 Modelled Air flow in the test

Due to the off centre placing of the concrete blocks a 2D model cannot be applied directly because the flow of air in the outer gap will be non-symmetrical. Therefore a 3D model was created to calculate the air flow in the outer gap uncoupled from the thermal problem. Although the Richardson number (approximately 0.4) suggests that natural convection cannot be totally neglected, this approach of separating the thermal problem from flow problem should be a good approximation since the result does not differ much from the rotational symmetric models in Section 4.4 in which coupled models are used. In the model the blocks were placed off centre with approximately 20 mm which rendered the minimum size of the gap to approximately 30 mm and the maximum size of 70 mm which is in good agreement to what was observed when the test was assembled. A more detailed view of the model is shown in Figure 4-7.

The flow calculation showed that the flow conditions for the sensors are different. The flow will have an impact on the modelling since the temperature gradient in the axial direction will be bigger if the air flow in the outer gap is smaller.

From Figure 4-8 it can be seen that the air flow from the inlets went straight down until it hit the bottom of the deposition hole and then bounced back up again. The non-symmetrical placing of the inlets and the off centre placing of the concrete block gave a very uneven air flow. Even if the inlets were placed symmetrical some kind of nozzle should be placed on the inlet to disperse the air to get a more even air flow. In Figure 4-9 the velocity profile is shown in the places where sensors were placed.

### 4.3.4 Heat flow modelling

To simplify the heat flow calculation an analytical expression that describes the laminar flow in the outer gap, Equation (4-11), was constructed. This was done because the 3D flow calculations are very time consuming. The analytical solution is compared to the numerical in Figure 4-10 and shows good agreement.

$$r \frac{d^2 v}{dr^2} = \frac{c}{\mu} \quad (4-11)$$

With the analytical expression for the air velocity in the outer gap the temperature in the deposition hole for the test was calculated, Figure 4-11.

To see how well the model works the modelled values are compared with data from the test. The model can predict the temperature and relative humidity in the test well. However, there are some uncertainties. Inner air gaps in the canister affected the final result. The thermal conductivity of the rock also needs to be quite high to get a good fit with experimental values.



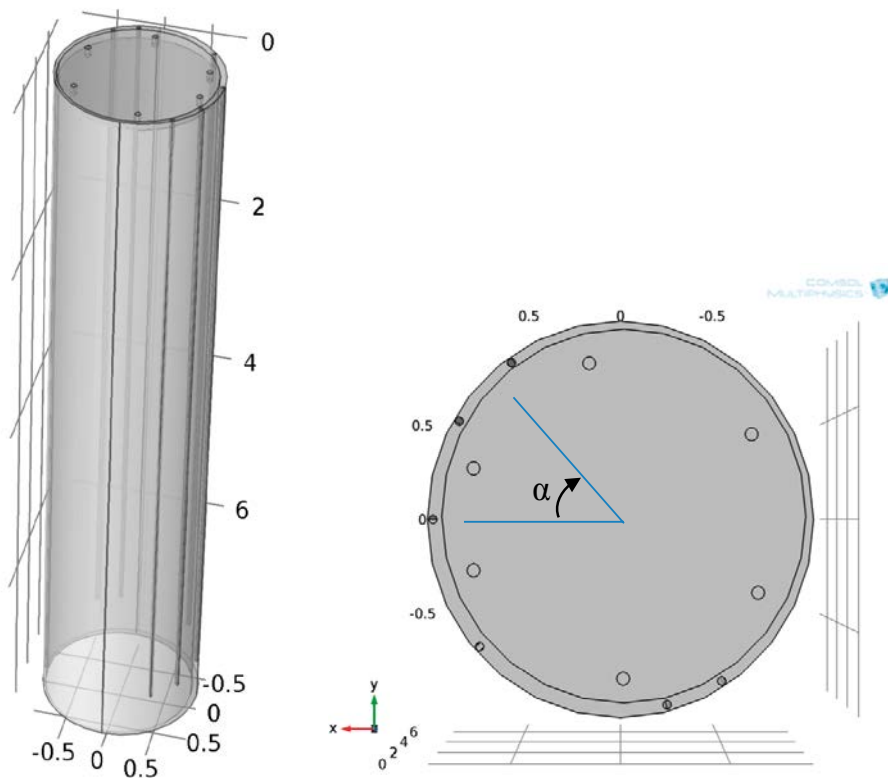


**Figure 4-7.** Geometric model use in flow calculations.

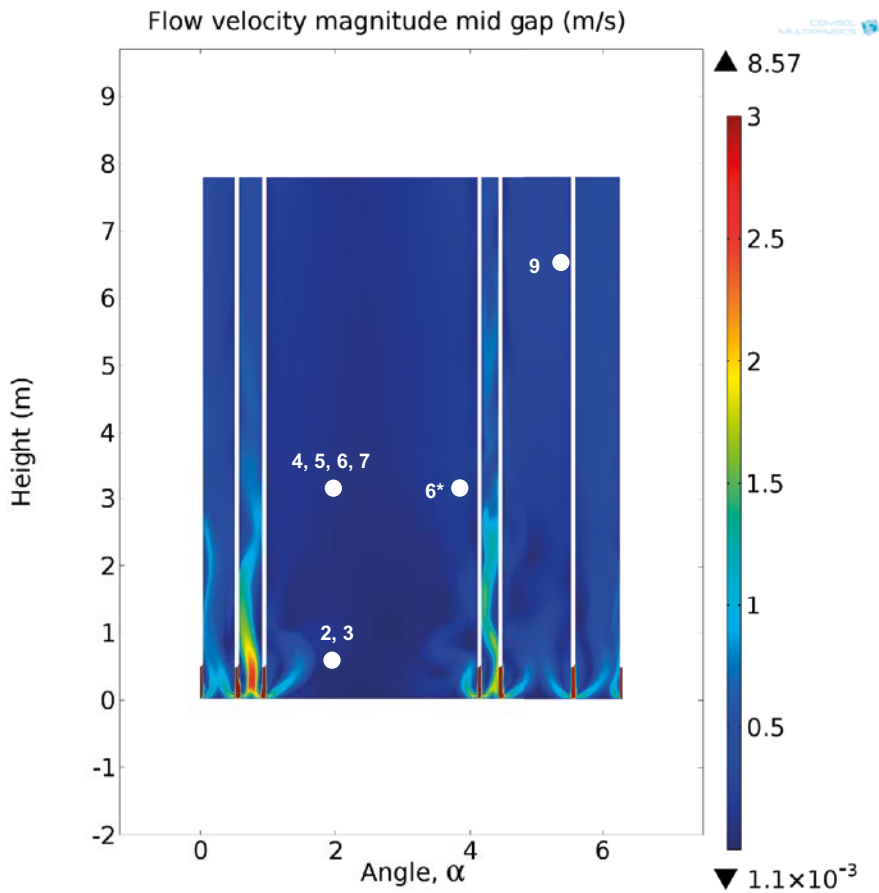


**Figure 4-8.** Modelled flow velocity in the middle of the outer gap at a total flow of 200 m<sup>3</sup>/h. White dots represent approximate placement of sensors. The graph shows a point in time for a time dependent solution.

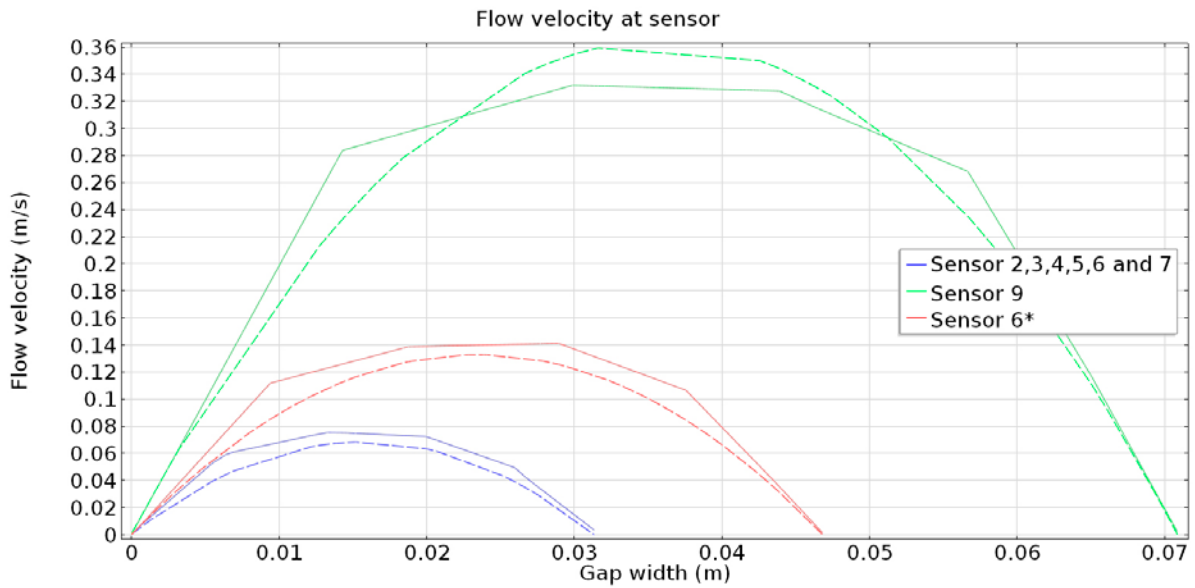


**Figure 4-9.** Modelled flow velocity across the outer gap in the places where the sensors were located.

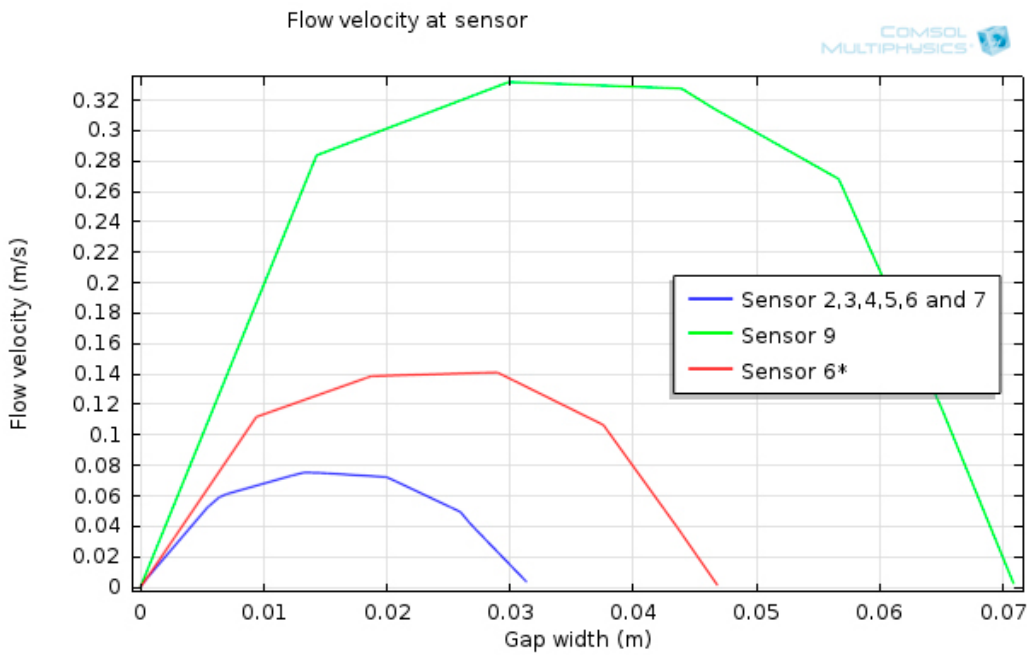


**Figure 4-10.** Velocity profile calculated numerically, solid lines compared to analytic solution, dashed lines at the location of the sensors.

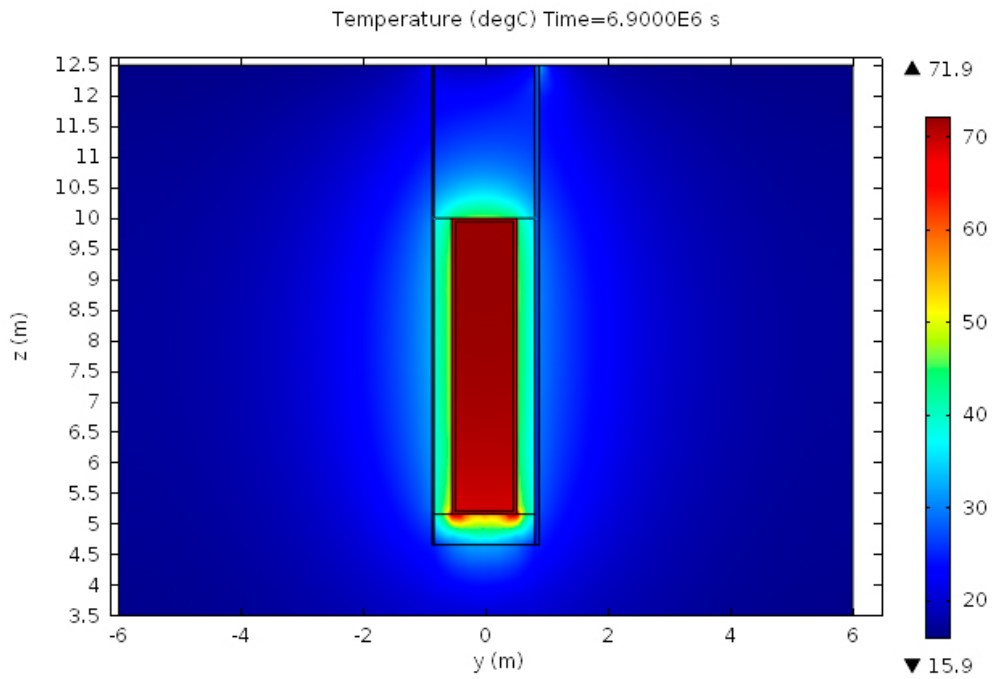


Figure 4-11. Modelled Temperature distribution at the end of the test.

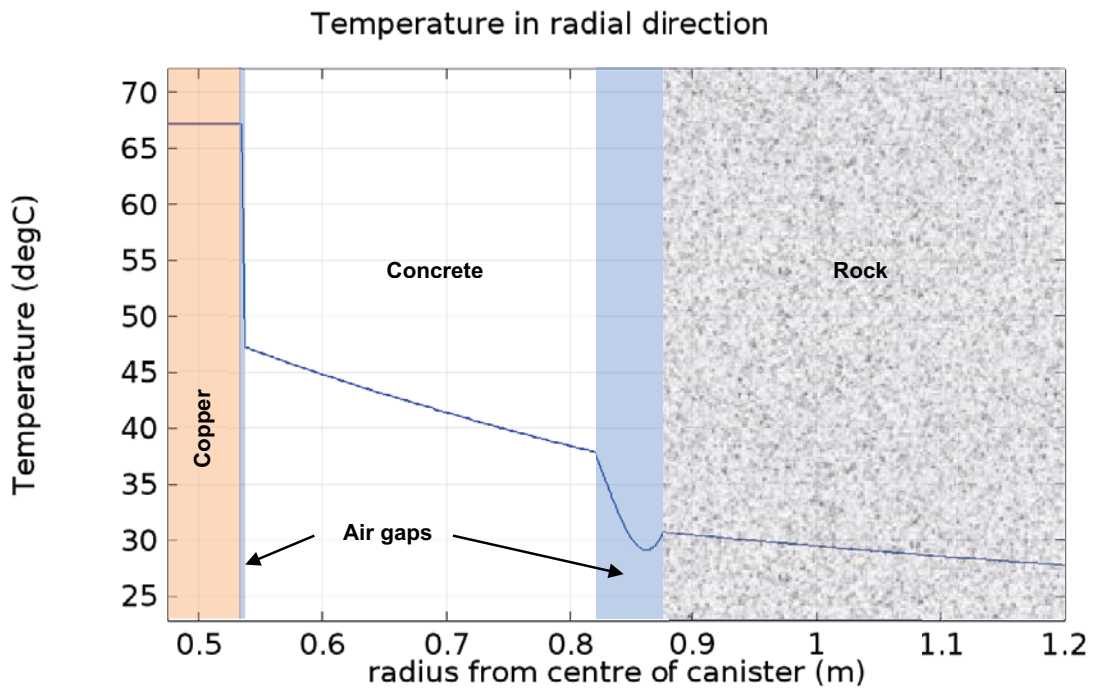
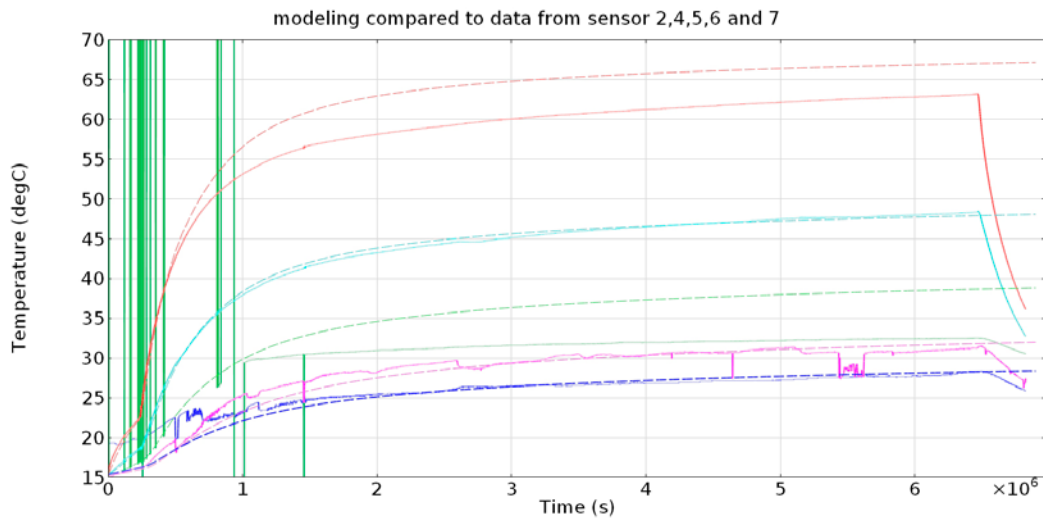
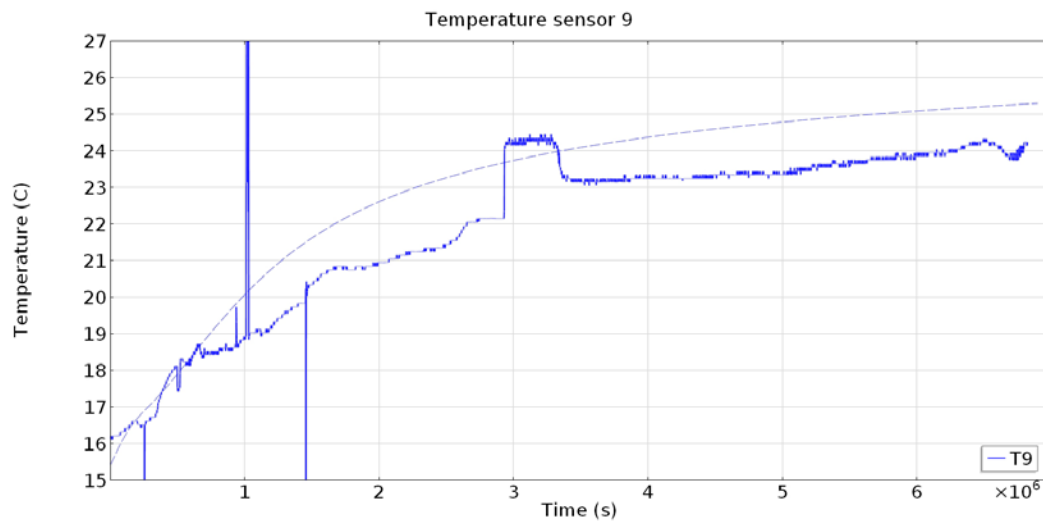


Figure 4-12. Modelled radial temperature profile at canister mid height.

In Figure 4-13 to Figure 4-15 it can be seen that all the values of the sensors were replicated with good accuracy except for sensor 4. This is probably because thermal radiation and convection was not considered in the inner gap between the canister and the concrete blocks in this model.



**Figure 4-13.** Data from sensors (solid lines) compared to modelled result (dashed lines). (sensor 2: blue, sensor 4: red, sensor 5: light blue, Sensor 6 and 6\*: green, sensor 7: magenta).



**Figure 4-14.** Temperature of sensor 9 (solid line) compared to modelled result (dashed line).

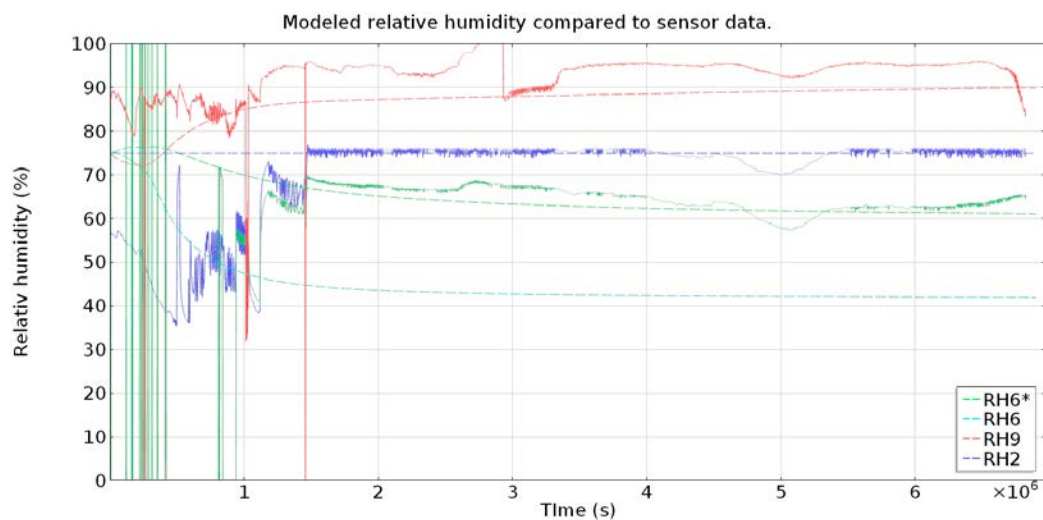


**Figure 4-15.** Relative humidity data (solid lines) compared to modelled results (dashed lines). Note that the modelled value 6\* is placed where sensor 6\* is believed to be, since placement is not completely known.

## 4.4 Modelling of a real case

To find out how a system with bentonite blocks would work this was modelled. For simplification a rotationally symmetric model was used. Dimensions and densities used are the same as in the reference design (SKB 2010).

Since it can take up to three month before the backfill is emplaced (Wimelius and Pusch 2008) the model covered the first 90 days after the canister has been deposited and used an air flow of 200 m<sup>3</sup>/h which enters the outer slot in the bottom. Four cases has been modelled, these are:

1. Model with air blown into the deposition hole with a relative humidity of 75 %.
2. Model with air blown into the deposition hole with a relative humidity of 85 %.
3. Model with air blown into the deposition hole with a relative humidity of 95 %.
4. Model with no air blown into the deposition hole with only free convection in the outer gap.

A big enough rock mass is used so that the heat will not affect the boundary during the time modelled. The rest of the boundary conditions are shown in Figure 4-16.

The model showed that due to the variations in temperature in axial direction the relative humidity decreased as the air was heated up. This means that there was a drying of the buffer for almost the whole deposition hole as can be seen in Figure 4-17.

To have something to compare to a deposition hole with current buffer protection or without buffer protection have also been modelled. The results are shown in Figure 4-18. The controlled atmosphere reduced the drying slightly. Also the top block in the current solution is in the risk of cracking in the horizontal direction which could cause some heaving. However, the differences are small. In the drying areas the cracking of the block will most likely take place in the radial direction and the risk of material falling out into the outer gap and heaving of the blocks are low.

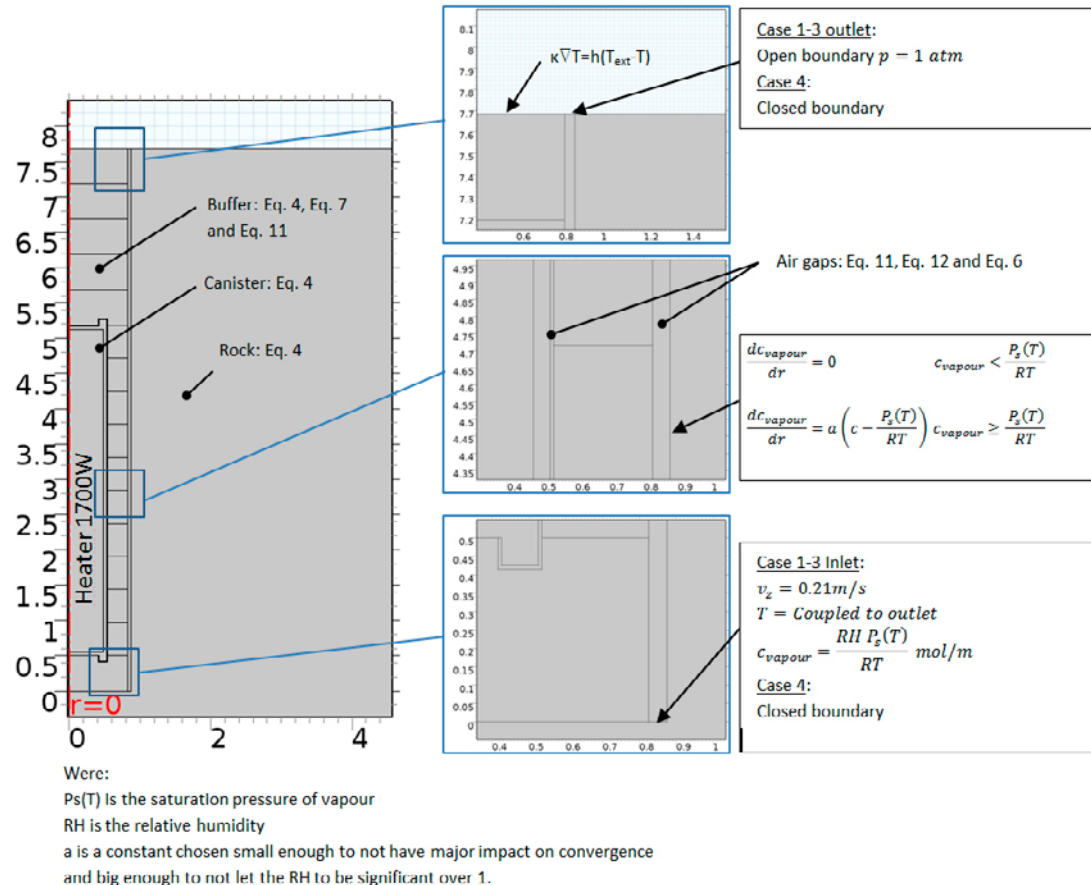
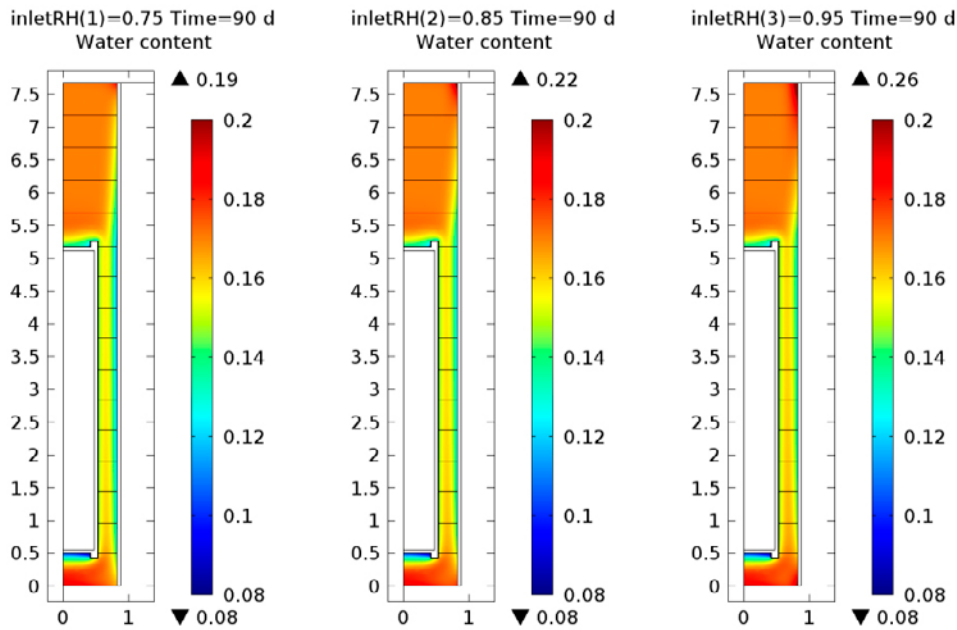
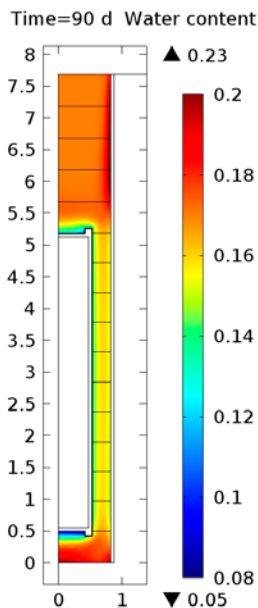


Figure 4-16. Boundary conditions and equations used for the modelling.



**Figure 4-17.** Case 1-3, water content after 90 days with 75, 85 and 95 % relative humidity in the air inlet. Initial water content was 17 %.



**Figure 4-18.** Case 4, modelled water content in the current reference design.

Equation (3-2) was used to predict the crack depth. The model indicated that the cracks go all the way through the buffer block after approximately 70 days, see Figure 4-19, if a thermal expansion coefficient of  $2.5 \times 10^{-4} \text{ K}^{-1}$  was assumed. The difference was not big if the relative humidity in the incoming air was varied between 75 % and 95 %. When blocks are cracked all the way through the inner and outer gap is connected and air can start to flow between them. This will accelerate the drying process. This was not covered by the model and it is therefore likely that the drying will go further than indicated by the model. The crack model also predicted a total crack width at the inner radius of approximately 43 mm which seems reasonable when looking at results from earlier test done with heaters (Johannesson et al. 2014), Figure 4-20.

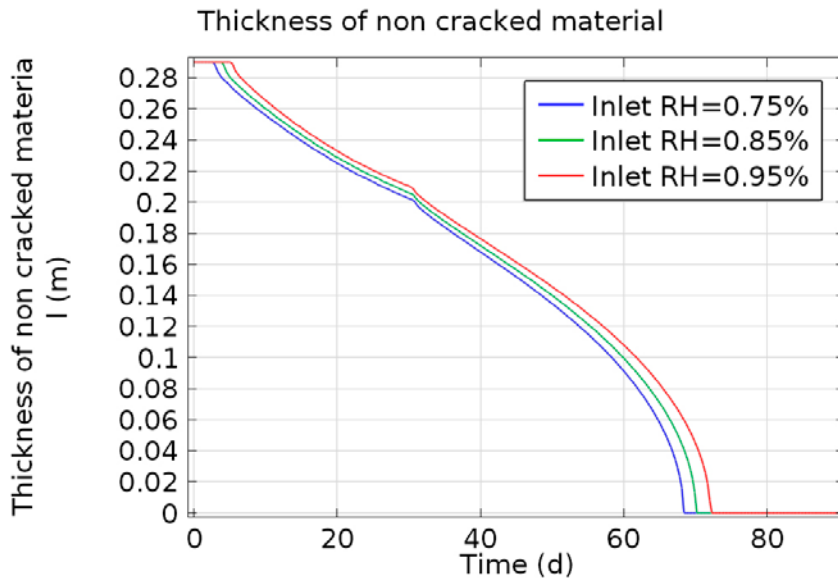


**Figure 4-19.** Model of how the zone with non-cracked material changes with time. After approximately 50 day the zone thickness is zero which means the cracks pass all through the material.



**Figure 4-20.** Cracking on the inside diameter of a buffer ring used in a heater test in Johannesson et al. (2014).

## 4.5 Possible improvements

Since the system is not very sensitive to the relative humidity in the air blown into the deposition hole, as seen in Figure 4-17, it would probably work to just blow down from the tunnel directly without the use of a dehumidifier if the relative humidity in the tunnel is 70 % or more. This method would be much simpler because only a fan and hoses down to the bottom would be needed. The air flow would still reduce the axial temperature gradient which causes high water content in the surface on the blocks on top of the canister, which is the case when free convection is the main process in the outer gap as seen in Figure 4-18.

This method could be an advantage if cooling of the rock wall would be needed to avoid spalling before the outer gap could be filled with pellets.





## 5 Coating of blocks

### 5.1 General description

The idea with this solution is to place a thin layer of a material that stops or reduces the water absorption or desorption rate. This will be equivalent to having a buffer protection in contact with the buffer. The advantage with this is that there will be no condense of water in the outer gap. Many different methods exist to add coatings. Before the work started possible coating methods had been identified. The coating methods that were considered were thermal spraying and adding degradable polymer with the help of solvents. Preliminary test were done and they showed that the solvents used for the degradable polymer also affected the bentonite surface causing bubbles underneath the coating. Thermal spraying was tested with zinc worked better and produced a relative crack free coating that could reduce the uptake of water significantly. However, the coating was quite thick, approximately 0.5 mm, and optimization was needed. This work has therefore focused on thermal spraying because it worked well and got good adhesion in the preliminary test and the method is also easy to scale up to full scale with existing equipment. New materials were tested in this work and an attempt to optimize the process parameters to reduce the thickness was done.

### 5.2 Materials tested

A number of materials were chosen to do test with these materials are:

- Aluminium oxide.
- Aluminium oxide with an organic sealant.
- Aluminium oxide with a zinc primer.
- Zinc.
- Copper.
- Copper-iron alloy.
- Polyethylene.

It was decided to test if the buffer blocks could be coated and if the coating would have the desired effect at this stage. Therefore, these materials have not been evaluated for how they will behave in a final repository. The reason why these materials were selected for testing is listed below.

#### ***Aluminium oxide***

Aluminium oxide was chosen because the material is naturally found in bentonite, therefore the material is not expected to influence the long-time safety in a negative way. However the aluminium oxide is very brittle and therefore it was decided to also seal possible cracks with a organic sealant. The sealant used was a commercial sealant based on epoxy which is used to seal thermal sprayed coatings. It was also believed that zinc could be used as a primer to increase adhesion.

#### ***Zinc***

Zinc was chosen because it normally has good adhesion and the residual stresses are low compared to some other metals

#### ***Copper***

Due to the fact that copper is already present in the deposition hole it was assumed that this material could fulfil the requirement on long-time safety. A copper iron alloy was also chosen to try and reduce the residual stresses that could cause the coating to crack.

### **Copper-iron ally**

This material was expected to have low residual stress and if is therefore likely to produce crack free coating.

### **Polyethylene**

Polyethylene is not an inorganic material but it can be applied at a relative low temperature and the material is very ductile which will protect the coating from cracking.

## **5.3 Coating of the samples**

The coatings were applied with a spray gun mounted on an industrial robot, see Figure 5-2. With this setup process parameters like the spray guns velocity relative to the sample and the distance from the gun to the sample could be controlled. The process parameters were adjusted for each material until a coating with good quality, i.e. a crack free surface with good adhesion, was achieved. In some cases the coating peeled off when the process parameters were outside the optimal interval. The thicknesses of the coating that were deemed to good enough for testing are shown in Table 5-1.

**Table 5-1. Thickness of coating.**

Coating material	Thickness ( $\mu\text{m}$ )	Additional information
$\text{Al}_2\text{O}_3$	60	
$\text{Al}_2\text{O}_3$ + sealent	60	Thickness of the sealent was not assessable
Zn + $\text{Al}_2\text{O}_3$	n.a.	The Zn layer partially peeled off when the top coat was sprayed, Which prevented also formation of a proper and even $\text{Al}_2\text{O}_3$ layer
Polyethylene	200	
Cu	90	
Cu	130	Optimized thickness for Cu was 130 $\mu\text{m}$
Cu	180	



**Figure 5-1.** A small scale bentonite block coated with copper.



*Figure 5-2. Robot with thermal spray gun used to coat the samples.*

#### **5.4 Testing of the coatings**

To test the performance of the coatings the coated samples were placed in an environment with a relative humidity of 95 %. The weight of the samples was measured with regular intervals and the result is plotted in Figure 5-3. Due to the fact that the samples have been handled in different environments and been subjected to different thermal loads it is expected the water content could be slightly different between the samples. Since the suction of the bentonite is a function of water content, lower water content will result in a higher suction for the bentonite. Therefore, the water content was measured after the test to get the final water content. From these values the initial water content was calculated. All of the coatings seem to have lost their effect after a relatively short time. The exception was the polyethylene which keeps its water tightness. The reason is probably that water enters through small cracks or pores and then the bentonite starts to swell which causes more cracks in the coating.

## 5.5 Modelling of a buffer stack with coating

To find out how water would redistribute in a buffer protected by a totally impermeable coating a modelling was done. The modelling was similar to the case 4 in Section 4.4 except a barrier impermeable to water vapour was added on the outer surface of the buffer blocks. The result is shown in Figure 5-4 and 5-5, and the modelling suggests that the water content will increase from 17 % to approximately 19 % due to the thermal gradient. The inner parts will dry and water will be redistributed from the inner parts to the outer surface of the buffer blocks.

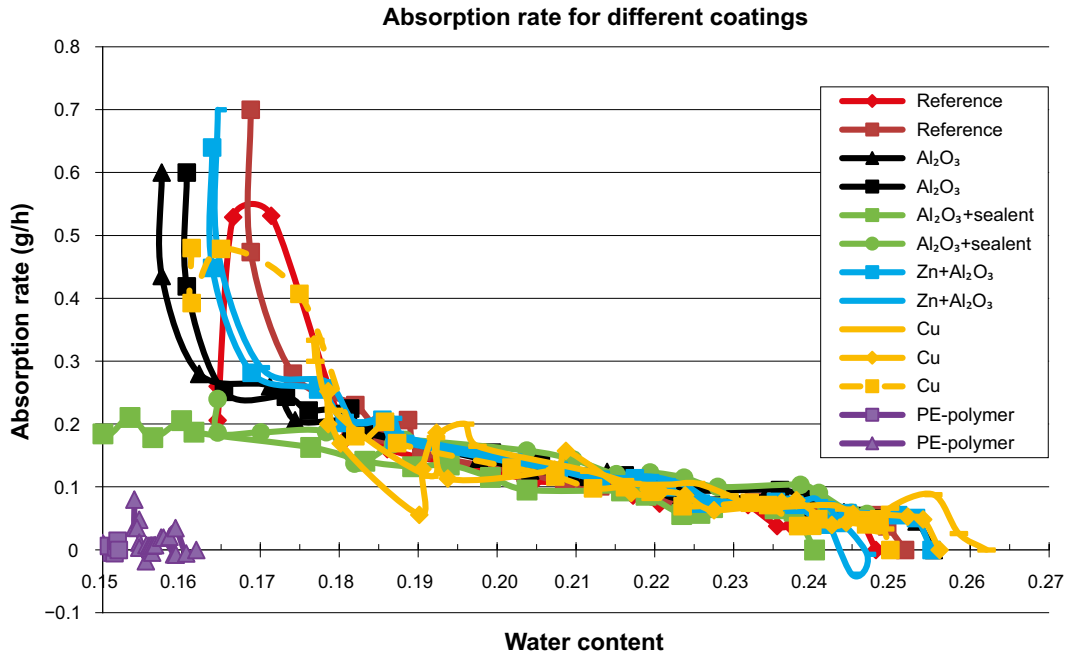


Figure 5-3. Absorption rate for different coatings.

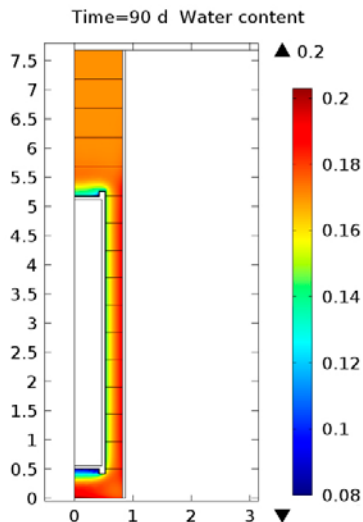
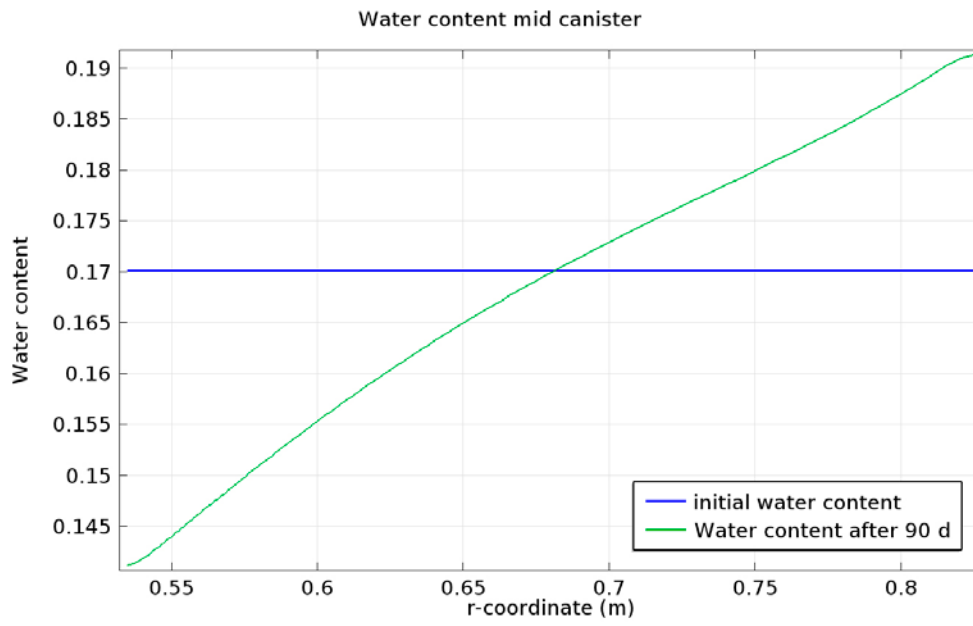


Figure 5-4. overview of the water content after 90 days.



*Figure 5-5. Modelled water content profile at mid canister height.*



## **6 Conclusions**

### **6.1 Controlled atmosphere**

Due to the axial heat gradient in the buffer it is difficult to even out the temperature, even when the flow of air is rather high. This causes drying in most places and wetting in some places. Overall the system does not perform much better than a buffer without any protection. Also the complexity increases because dehumidifier, fans, and control system are needed. Although the system could probably be simplified it is still more complex than the current solution.

No or very little heaving is expected due to the fact that the buffer mainly dries. Also the drying conditions also results in small risk of pieces falling out in the outer gap. However, because it is expected that crack all through the buffer blocks will form it could be such large drying that the block cracks also in horizontal direction. If this would happen pieces could fall into the outer gap.

The method is also quite sensitive to eccentric placement of the buffer blocks in the deposition hole.

Therefore it is recommended that other solutions are investigated to find a method for protecting the buffer that is less complex.

### **6.2 Coating of blocks**

The coatings tested are quite brittle and will crack after small increases in water content with exception for the polyethylene. It is expected that the water content will increase in the outer part of the block close to the coating when a thermal gradient is applied over the block. This will make the coatings crack due to the low ductility and their function will be lost. This was never tested since the coatings were more porous than expected and cracked already after a small amount of water had passed through them.

In the case of a ductile coating like Polyethylene there is a significant risk that the water content in the outer diameter increases so much that the blocks start to crack in the horizontal direction. This horizontal cracking would cause heaving.

The conclusion is therefore that the coating would have no major improvement at best and could even be worse than current solution if a ductile and non-permeable coating is used.

Coating of the blocks would also make the manufacturing process more complex and put high demands on handling and quality control to ensure that the coatings were not damaged during transport and installation.

The recommendation is therefore not to continue to investigate this alternative for the protection of the buffer when conditions are such that the buffer is drying.





## References

SKB's (Svensk Kärnbränslehantering AB) publications can be found at [www.skb.com/publications](http://www.skb.com/publications).

**Johannesson L-E, Kristensson O, Åkesson M, Eriksson P Hedin M, 2014.** Test and simulations of THM processes relevant for the buffer installation. SKB P-14-22, Svensk Kärnbränslehantering AB.

**Sandén T, Börgesson L, 2010.** Early effects of water inflow into a deposition hole. Laboratory tests results. SKB R-10-70, Svensk Kärnbränslehantering AB.

**Sandén T, Nilsson U, Andersson L, 2016.** Investigations of parameters influencing bentonite block quality. Laboratory investigation. SKB P-16-06, Svensk Kärnbränslehantering AB.

**SKB, 2010.** Design, production and initial state of the buffer. SKB TR-10-15, Svensk Kärnbränslehantering AB.

**Wimelius H, Pusch R, 2008.** Buffer protection in the installation phase. SKB R-08-137, Svensk Kärnbränslehantering AB.

**Åberg A, 2009.** Effects of water inflow on the buffer – an experimental study. SKB R-09-29, Svensk Kärnbränslehantering AB.

**Åkesson M, Börgesson L, Kristensson O, 2010.** SR-Site Data report. THM modelling of buffer, backfill and other system components. SKB TR-10-44, Svensk Kärnbränslehantering AB.

SKB is responsible for managing spent nuclear fuel and radioactive waste produced by the Swedish nuclear power plants such that man and the environment are protected in the near and distant future.

**skb.se**